JETIR.ORG ISSN: 2349-5162 | ESTD Year : 2014 | Monthly Issue
JOURNAL OF EMERGING TECHNOLOGIES AND INNOVATIVE RESEARCH (JETIR)
An International Scholarly Open Access, Peer-reviewed, Refereed Journal

"Detection and Classification of Power Quality Disturbances Using S-Transform Features and an Artificial Neural Network"

Prof.P.S.Ganorkar pratyanjasganorkar@gmail.com
Phd.Scholar
Electrical Engg Dept.
MGICOET , Shegaon
Maharashtra, India

Dr.M.A.Beg ansarbeg@gmail.com
Professor
Electrical Engg Dept.
, Shegaon Maharashtra,
India

Dr.V. A. Ghodeswar ghodeswarvaibhav@gmail.com
HOD
Electrical Engg Dept.
MGICOET , Shegaon
Maharashtra, India

Prof.R.R.Deotare roshan.deotare99@gmail.com
Phd.Scholar
Electrical Engg Dept.
MGICOET , Shegaon
Maharashtra, India

Abstract

Power quality disturbances (PQDs) can influence the behavior of electrical power systems and the sensitive end-user equipment operating within them. In this paper, a signal processing and machine learning-based technique is considered for identification of voltage disturbances based on the use of the Stockwell transform (S-transform) and artificial neural network (ANN). A MATLAB/Simulink model of the IEEE 14-bus benchmark system is provided as the platform of simulations. Representative examples of time-domain waveforms for normal operation, an interruption-labeled event, and a voltage sag labeled event are analyzed along with the S-transform magnitude plots and frequency-dependent time contours for these voltage waveforms. The normal case shows almost stationary magnitude at the fundamental frequency, while the two disturbance cases have localized decrease of the 50 Hz component magnitude and brief high-frequency activity near the borders of the events. According to the reported results of classifier comparison, the ANN demonstrates the accuracy of 91.00%, then k-nearest neighbors and support vector machine – 81.25%, and random forest and decision tree classifiers – 75.00%. It is shown that S-transform provides informative time-frequency characteristics for PQD identification. More details about the dataset, extracted feature vector, ANN architecture and testing process are needed.

Index Terms— Artificial Neural Network, IEEE 14 bus system, power quality disturbance, S Transform, Stockwell Transform, voltage interruption, voltage sag.I. INTRODUCTION

Power Quality (PQ) monitoring is necessary for a power system in order to maintain good power quality. Increased use of power electronic interfaces, non-linear loads, Distributed Energy Resources (DER), and sophisticated industrial devices has further increased the significance of monitoring disturbances. Voltage sag, swell, interruption, harmonics, flicker, and impulsive or oscillatory transient are some of the common PQ phenomena. Such disturbances may cause equipment malfunctions, false tripping, production downtimes, and poor service continuity. IEEE Std 1159 defines the terminology used in PQ and offers recommendations regarding PQ monitoring [1].

Traditional waveform measurement and RMS analysis are appropriate to determine the magnitude and duration of disturbances. Nevertheless, in some cases, where the signal has abrupt changes or higher frequencies are overlaid on them,

time-frequency analysis may be necessary to complement traditional approaches. The Stockwell transform has time-localization capabilities based on frequency information and an amplitude-phase representation, being ideal for non-stationary voltage signals analysis [2]. Some studies have analyzed S-transform properties along with probabilistic neural networks and ANN classifiers [4].

These voltage traces are analyzed in this paper based on their instantaneous waveforms, S-transform magnitude distributions, and time contours. The results of classification accuracy of five different machine learning techniques, namely RF, KNN, ANN, SVM, and DT, are compared. Of special interest is the analysis of visible signal properties and the separation of the observed results from methodology aspects which are not entirely described in the existing experimental record [3]

II. SIMULATION MODEL AND CLASSIFICATION METHODOLOGY

Objective of the study includes (i) description of the IEEE 14 bus system simulation model employed for obtaining typical voltage disturbance signals; (ii) comparison of normal,

sag-marked, and interruption-marked three-phase waveforms; (iii) analysis of fundamental frequency components and transients using S transform method; and (iv) validation of the performance of five machine learning classifiers. Contribution of the study lies in an integrated assessment of voltage waveform signals, time frequency representation, and classifier level performance of the concerned disturbances.

III. SIMULATION MODEL AND CLASSIFICATION METHODOLOGY

A. IEEE 14-Bus Simulation Model and Signal Acquisition

Modeling of IEEE 14-Bus Test System in MATLAB/Simulink involves buses that are interconnected by transmission line impedances, generators, loads, and reactive power compensation components, as illustrated in Fig. 1 below. The Simulink model serves to provide a power system model that can be used to observe voltages in the power system during steady-state and disturbance conditions. This analysis is mainly based on three-phase voltage waveform as well as the digitized signals provided in the results. The disturbances in this model are not explicitly indicated.

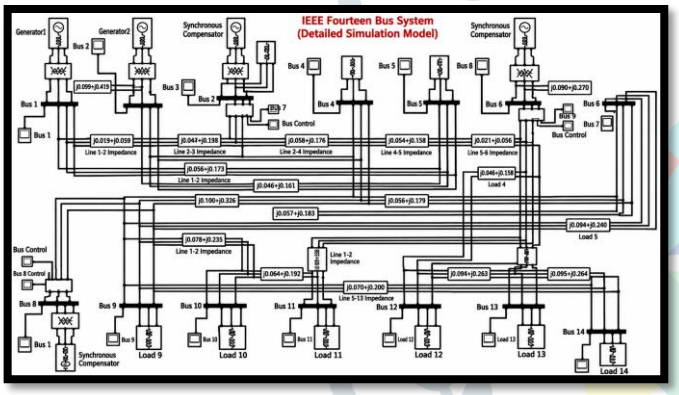

Fig. 1. MATLAB/Simulink schematic of the IEEE 14-bus power-system model.

The displayed voltage signals span a range of about 0-0.12 seconds. There needs to be a reproducible protocol for data acquisition and pre-processing in order to conduct an experiment for classification using the S-transforms. The data acquisition and pre-processing protocol should include the sampling rate, time interval for recording, bus and phase considered, per-unit system, time of disturbance onset and clearing, and normalization method. The feature scaling method should only be applied to the training data.

B. S-Transform-Based Time–Frequency Analysis

The S-transform is an approach for representing the time-varying signal by a Gaussian window function whose effective width varies according to the frequency component. The S-transform achieves good frequency resolution at lower frequencies and good time localization at higher frequencies.. For a continuous-time signal x(t), the transform is defined as [2]

$$S(\tau, f) = \int_{-\infty}^{\infty} x(t) \cdot |f|/\sqrt{(2\pi)} \cdot \exp[-f^2(\tau - t)^2/2] \cdot \exp(-j2\pi ft)\, dt, \quad f \neq 0. \quad (1)$$

where, τ is the time shift factor, f represents frequency, and j is the imaginary number. The absolute value $|S(\tau,f)|$ represents a time-frequency distribution that allows any variations in the fundamental components and transient spectrum to be detected. For the 50 Hz system illustrated in the provided figures, we have fundamental frequency curve and high frequency curve respectively defined by

$$C_{50}(\tau) = |S(\tau, 50\ \text{Hz})|, \quad H_{200}(\tau) = \max\{\, |S(\tau,f)| : f \geq 200\ \text{Hz}\,\}. \quad (2)$$

The 50 Hz contour gives indication about the timing and amplitude of the voltage disturbance, while the high-frequency contour gives indication about the spectral activity near sudden transitions. The contours give information on the transform magnitudes and must not be directly related to any per unit RMS value without a proper calibration process.

C. Feature Extraction

The S-transform coefficients can be condensed to form a feature vector prior to machine learning for classification. Some possible features that may be used for classification purposes include the mean and standard deviation of the contour of fundamental frequency, the minimum value of the fundamental magnitude, the time when the minimum occurs, the total energy of the transform, the maximum value of the high-frequency magnitude, and statistical features like mean, standard deviation, and spectral entropy[9].

The original experiment is described as using S-transform-derived statistical features; however, the exact feature definitions, number of attributes, and extraction settings underlying the reported 91.00% ANN accuracy are not available. As such, the terms included herein must be seen as technologically sound examples, and not as the reconstructed version of the input feature matrix.

D. ANN-Based Classification and Comparator Models

The classification process includes acquisition of the waveforms, preprocessing, S-transform calculation, feature extraction, and classification via a supervised learning approach. An input feature vector is mapped into class scores via ANN's weights, bias factors, and nonlinear functions of neurons' activity. The predicted class of the disturbance is obtained via the ANN output. Algorithms KNN, SVM, RF, and DT are considered as comparative models based on the performance measures given in the results.

Fair model comparison needs identical training samples and the same test protocol. For example, it is necessary to describe the feature selection method, size of layers of ANN, training algorithm, number of epochs, hyperparameter tuning, number classes, and split into training-validation-test sets. All these model parameters that differ from those used in the original article are unknown.

E. Classification Performance Measure

Accuracy of the overall classification is computed as the percentage of test data that have been classified into their proper classes:

$$\text{Accuracy (\%)} = \text{Number of correctly classified test data/Total number of test data} * 100 \quad (3)$$

In the case where the frequency distribution of disturbance classes is not equal, accuracy alone would be inadequate as an assessment metric. Other metrics such as the confusion matrix, precision, recall and F1-score should be used. The classifier figure above shows overall accuracies but no predictions.

IV. RESULTS AND DISCUSSION

A. Normal Operating Condition

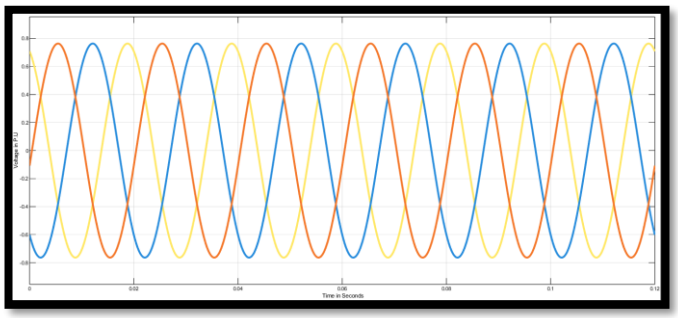

Fig. 2. Three-phase voltage waveforms under the normal operating condition (0–0.12 s).

As depicted in Fig. 2, the three phases are almost sinusoidal and balanced with constant amplitude in all cycles during the time span considered. The period for each cycle is around 0.02 s, matching with the nominal frequency of 50 Hz. The peaks are nearly ±0.75 – 0.80 p.u., visually obtained from the graph. This wave form acts as the base for analyzing the variations due to the two disturbances presented.

B. Interruption-Labelled Voltage Disturbance

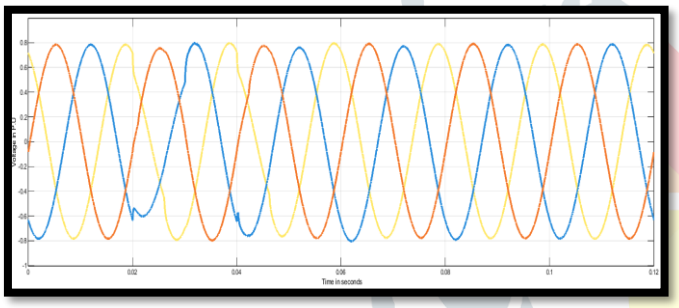

Fig. 3. Three-phase voltage waveforms for the interruption-labelled disturbance.

Figure 3 depicts a deviation in the normal sinusoidal shape at around 0.02 s, the most noticeable one occurring in one of the phases plotted. This deviated phase has a short dip and distortion in the instantaneous voltage prior to restoring back to the normal sinusoidal shape. The digitized trace chosen in Fig. 5 contains a nearly flat line for some part of the duration of the event. Since there is no voltage loss in all the phases at once, the record is called an interruption labeled or phase selective disturbance.

C. Voltage-Sag-Labelled Disturbance

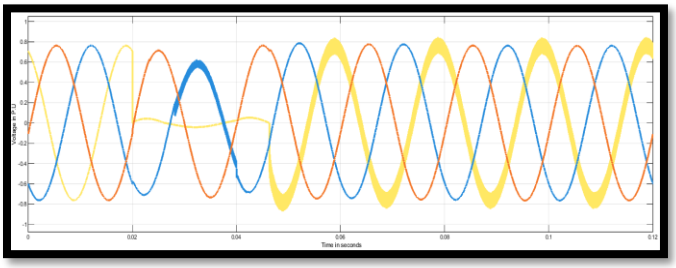

The waveform with “voltage sag” label in Fig. 4 displays considerable decrease in instantaneous value of one phase starting from approximately 0.02 s up to the time period of 0.04 to 0.05 s. Traces of other phases demonstrate oscillation behavior but display certain changes as well. Another signal taken for digitalization in Fig. 5 is characterized by voltage sag over similar period of time. However, it should be clearly defined measurement window and criteria for voltage retention in order to define event[4].

Fig. 4. Three-phase voltage waveforms for the voltage-sag-labelled disturbance.

D. Interpretation of S-Transform Magnitude Maps and Contours

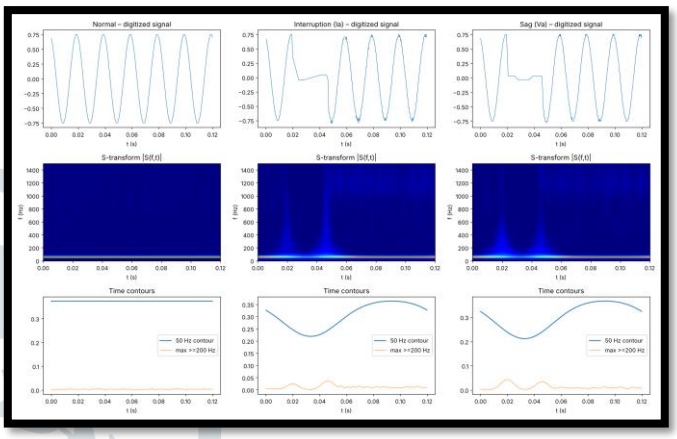

Fig. 5. Digitized signals (upper row), S-transform magnitude maps (middle row), and time contours at 50 Hz and ≥200 Hz (lower row), for normal, interruption-labelled, and sag-labelled conditions.

Figure 5 displays three kinds of signal representation of the normal condition and those two with disturbances labeled. According to the digitized waveforms, the normal signal represents the repetitive sinusoidal waveform. In both disturbed waveforms, there appears a distinct decrease in the selected channel in the time range from about 0.02 seconds to 0.045-0.05 seconds. The commonality of these decreased voltage intervals underscores the significance of well-defined events and proper multi-feature discrimination.

The magnitude maps of the S-transform cover the range of frequency from about 0 to 1.5 kHz. For the normal state, the principal spectral response is mostly seen in the vicinity of the fundamental frequency range and with little time variation. In both disturbed cases, the localized variations at the onset and clearing moments of the event can be seen, along with other high-frequency spectral responses [7]. Due to lack of calibration of magnitude color bar, the exact magnitude of spectra can’t be derived from the above maps.

The bottom plots of Fig. 5 are the 50 Hz magnitude contour and the peak magnitude for above approximately 200 Hz. In case of normal operation, the 50 Hz contour stays constant at the level of 0.38 on the scale of transform, while the high frequency contour stays close to zero. In case of interruption, the 50 Hz contour decreases to the level of approximately 0.22 within 0.03 seconds, then returns back. The sag plot has the same type of decrease, reaching the value of approximately 0.21 at 0.035 seconds. Peaks appear on the high frequency contours at the apparent beginning of events, at approximately 0.02 and 0.045 seconds. These values are only rough visual estimates and are not taken from any numeric data set.

It can be seen that the S-transform representation contains information about the start time, duration, relative magnitude

and frequency content during transition. However, these two event labeled contours are similar enough that reliable classification will require precise RMS based labeling, the phase or bus to be considered and other statistical measures.

E. Comparative Performance of Machine-Learning Classifiers

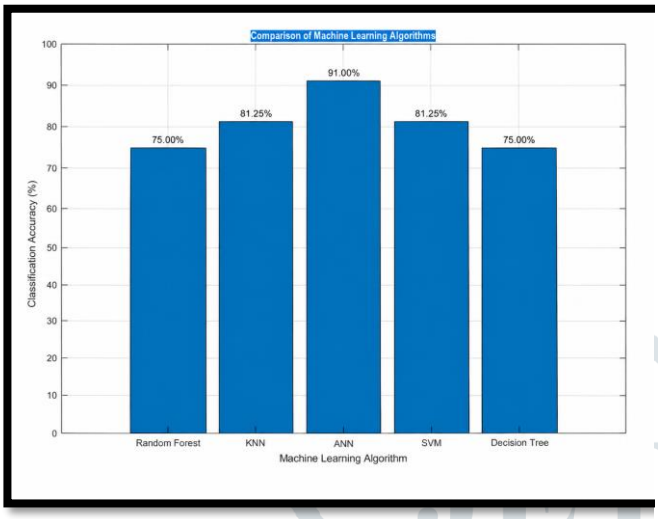

Fig. 6. Comparison of reported classification accuracies for RF, KNN, ANN, SVM, and DT.

The accuracies of classification reported for Fig. 6 are shown in Table I. The highest value of accuracy is obtained from ANN with 91.00%. The accuracies of KNN and SVM are equal to 81.25%, while those of RF and DT are 75.00%. This indicates that the highest accuracy by ANN is 9.75% greater than the second highest accuracy and 16.00% greater than those of RF and DT.

TABLE I. REPORTED CLASSIFICATION ACCURACY OF THE FIVE ALGORITHMS

Classification algorithm	Reported accuracy (%)
Random Forest (RF)	75.00
K-Nearest Neighbors (KNN)	81.25
Artificial Neural Network (ANN)	**91.00**
Support Vector Machine (SVM)	81.25
Decision Tree (DT)	75.00

As per the stated ranking, the performance of ANN with the current feature set is quite promising[6]. However, the lack of any information regarding the test set, feature matrix, tuning process, and confusion matrix makes any statistical comparison impossible. Nothing can be concluded from the total accuracy graph with respect to the sensitivity to single event detection, noise immunity, and performance in novel power grids.

F. Experimental Limitations

The experimental data is in the form of waveform graphs, S-transform plots, and accuracy comparison of classifiers. Critical reproducibility information such as number of records, class distribution, sampling rate, change in operating point, disturbance injection, selected voltage channel, definition of numerical features, ANN structure, random seed, and validation approach are not provided. Additionally, the interruption-labeled and sag-labeled instances all have periods of low instantaneous voltage. The experimental results thus need to be confirmed using RMS threshold definitions before releasing it for publication.

IV. CONCLUSION

In this paper, the detection and classification of power quality disturbances were investigated through the use of S-transform time-frequency analysis in combination with an ANN classifier based on voltage samples of representative nature with regard to an IEEE 14 bus MATLAB/Simulink model. The normal operation case results in the formation of stable three-phase sinusoidal voltage waveform and the constant contour of the fundamental frequency. At the same time, the examples labelled as sags and interruptions are characterized by the presence of time localized voltage drops and high-frequency content around the time of disturbance. These features highlight the usefulness of the S-transform for identification of time localized voltage changes which are not adequately expressed through time domain amplitude values. In the conducted comparison of five machine learning techniques, the ANN provided the highest classification accuracy equal to 91.00% and outperformed KNN and SVM (81.25%) as well as RF and DT (75.00%).

V. FUTURE SCOPE

Further research must consider swells in voltage, harmonic distortion, flicker, transient events, and concurrent disturbances. The proposed method should be tested against variability in the severity, duration, bus position, loading conditions, and signal-to-noise ratio of events. Precise documentation of the feature vector and artificial neural network hyperparameters, in conjunction with careful splitting of the dataset, would enhance reproducibility. Alongside total accuracy, confusion matrices, class-specific precision, recall, F1-scores, and uncertainty measures need to be reported. Lastly, the computation cost and effectiveness with measured waveforms in the field need to be considered for practical purposes.

REFERENCES

[1] IEEE Std 1159-2019, IEEE Recommended Practice for Monitoring Electric Power Quality, IEEE, 2019, doi: 10.1109/IEEESTD.2019.8796486.

[2] R. G. Stockwell, L. Mansinha, and R. P. Lowe, "Localization of the complex spectrum: The S transform," IEEE Transactions on Signal Processing, vol. 44, no. 4, pp. 998–1001, 1996, doi: 10.1109/78.492555.

[3] S. Mishra, C. N. Bhende, and B. K. Panigrahi, "Detection and classification of power quality disturbances using S-transform and probabilistic neural network," IEEE Transactions on Power Delivery, vol. 23, no. 1, pp. 280–287, 2008, doi: 10.1109/TPWRD.2007.911125.

[4] R. Kumar, B. Singh, D. T. Shahani, A. Chandra, and K. Al-Haddad, "Recognition of power-quality disturbances using S-transform-based ANN classifier and rule-based decision tree," IEEE Transactions on Industry Applications, vol. 51, no. 2, pp. 1249–1258, 2015, doi: 10.1109/TIA.2014.2356639.

[5] M. V. Reddy and R. Sodhi, "A modified S-transform and random forests-based power quality assessment framework,"

IEEE Transactions on Instrumentation and Measurement, vol. 67, no. 1, pp. 78–89, 2018.

[6] S. A. Kiranmai and A. Jaya Laxmi, "Data mining for classification of power quality problems using WEKA and the effect of attributes on classification accuracy," Protection and Control of Modern Power Systems, vol. 3, article 29, 2018.

[7] "Detection and classification of power quality disturbances based on improved adaptive S-transform and random forest," Energies, vol. 18, no. 15, article 4088, 2025.

[8] J. Li, H. Liu, D. Wang, and T. Bi, "Classification of power quality disturbance based on S-transform and convolution neural network," Frontiers in Energy Research, vol. 9, 2021.

[9] H. Wang, P. Wang, and T. Liu, "Power quality disturbance classification using the S-transform and probabilistic neural network," Energies, vol. 10, no. 1, article 107, 2017.

[10] M. Uyar, S. Yildirim, and M. T. Gencoglu, "An expert system based on S-transform and neural network for automatic classification of power quality disturbances," Expert Systems with Applications, vol. 36, no. 3, pp. 5962–5975, 2009.